

## Surface Modification of Stainless Steel-304 Electrode. 1. Voltammetric, Rotating Ring-Disc Electrode and XPS Studies

*Dražen Marijan,<sup>a,#</sup> Marijan Vuković,<sup>a,\*</sup> Petar Pervan,<sup>b</sup>  
and Milorad Milun<sup>b</sup>*

<sup>a</sup> *Center for Marine and Environmental Research, Ruđer Bošković Institute,  
P.O.B. 1016, HR-10000 Zagreb, Croatia*

<sup>b</sup> *Institute of Physics, P.O.B. 304, HR-10000 Zagreb, Croatia*

Received March 27, 1998; revised February 11, 1999; accepted April 12, 1999

Hydrous oxide film was grown on stainless steel-304 under conditions of cycling voltammetry in 1 mol dm<sup>-3</sup> NaOH solution. The anodic voltammetric peak of Fe(OH)<sub>2</sub> oxidation was used as a measure of the oxide growth as a function of potential limits, sweep rates and the number of potential cycles. The oxide film stability was monitored by the use of rotating ring-disc electrode. During potential cycling in alkaline solution, it was found that after 30 cycles, 1.4% of the anodic charge was due to iron dissolution from the oxide film. The selective dissolution of iron and nickel from the oxide film, previously grown in alkaline solution, was monitored at the potential of open circuit in an acid solution of pH 2.7. A model for enhanced stability of hydrous oxide film in acid solution is proposed. The model, based on voltammetric, rotating ring-disc electrode and X-ray photoelectron spectroscopy measurements, implies that after hydrous oxide growth by potential cycling in an alkaline solution, the oxide placed in an acid solution remains enriched in chromium due to selective dissolution of nickel and iron. The Cr-O-Cr chains stabilize the modified layer and contribute to the enhanced stability against corrosion. This model unifies several previously proposed models: the model for a hydrous oxide growth by

---

\* Author to whom correspondence should be addressed. (E-mail: mvukovic@rudjer.irb.hr)

# Present address: PLIVA d. d. Research Institute, B. Filipovića 25, HR-10000 Zagreb, Croatia

potential cycling, the polymeric hydrated oxide model for the passivity of iron and stainless steels and the percolation model for the passivity of stainless steels.

*Key words:* stainless steel-304, surface modification, voltammetry, rotating ring-disc electrode, X-ray photoelectron spectroscopy, oxide growth

## INTRODUCTION

Surface modifications of numerous transition metals (Ru, Ir, Rh, Fe, Ni, W) by the growing hydrous oxide films under conditions of repetitive potential cycling have received a great deal of attention mainly due to the improved electrocatalytic properties of single metals in the electrochemical oxygen evolution.<sup>1</sup> The question that intrigues us is to what extent iron and nickel would change their electrochemical activity when present in an alloy and under such experimental conditions in which an oxide would grow on a single metal. In other words, whether some synergetic effects could be found in a stainless steel. In this work, stainless steel-304 was used because of its importance as a constructive material in industrial equipment. Recent studies<sup>2,3</sup> on stainless steel-302 and inconel-600 show an enhanced resistance against corrosion under acid conditions upon the growth of hydrous oxide films in alkaline solutions.

In this work, we propose a model for the enhanced stability of modified oxide film. It is based on characterization of the alloy surfaces prior to and after the modification procedure. In this context we apply several experimental methods: cyclic voltammetry, rotating ring-disc electrode (RRDE) and X-ray photoelectron spectroscopy (XPS) in order to characterize the oxide film growth process and determine the stability of the grown oxide in acid solutions.

## EXPERIMENTAL

### *Working Electrodes*

Working electrodes, stainless steel-304 (Goodfellow, FeCr18Ni10) were either a wire (0.25 cm<sup>2</sup> geometrical area) fixed by epoxy resin into a glass tube, or a rod mounted into a PINE Mod. AFMT135PTPT rotating ring-disc electrode (RRDE) with interchangeable disc. The electrodes were driven by a PINE Mod. AFMSRXE rotator and controlled by a PINE Model AFRDE4E bipotentiostat. The stainless steel-304 rod (Goodfellow, FeCr18Ni10) was mechanically machined to appropriate dimensions to fit into the RRDE assembly. The geometrical surface area of the stainless steel-304 disc and the platinum ring were 0.2 cm<sup>2</sup> and 0.11 cm<sup>2</sup>, respectively. The electrode was rotated at 2500 rotations per minute (rpm).

The surface of the stainless steel-304 electrode was polished with emery paper and 0.05  $\mu\text{m}$  alumina powder, degreased by acetone, ethyl alcohol, and washed with quadruply distilled water. After these cleaning steps, the electrode was immediately immersed in the cell and polarized cathodically at  $-0.6\text{ V}$  vs. saturated calomel electrode (SCE) in  $0.5\text{ mol dm}^{-3}\text{ H}_2\text{SO}_4$  (Fluka *puriss. p.a.*) for 5 min. All potentials were referred to the SCE. A platinum foil was used as a counter electrode. The polishing procedure and cathodic polarization were repeated before each oxide film preparation.

### *The Experimental Procedure with RRDE*

The first step was the determination of active electrochemical potentials on the platinum ring electrode, where possible intermediates in electrochemical reactions can be detected. It is known that the enhanced stability of stainless steels against corrosion is due to chromium species, and that the process of passivity is accompanied by an enrichment in chromium.<sup>4</sup> Therefore, in this work attention was paid to dissolved iron and nickel species. Figure 1 shows the cyclic voltammogram on a platinum electrode of a mixture of  $\text{Ni}^{2+}$  and  $\text{Fe}^{2+}$  in  $0.5\text{ mol dm}^{-3}\text{ Na}_2\text{SO}_4$  (Kemika, *p.a.*) solution adjusted to pH 2.7 by addition of  $\text{H}_2\text{SO}_4$ . Two anodic peaks at  $-0.4\text{ V}$  and  $0.5\text{ V}$  correspond to  $\text{Fe}^{2+}$  and  $\text{Ni}^{2+}$  oxidation, respectively. The platinum background in  $0.5\text{ mol dm}^{-3}\text{ Na}_2\text{SO}_4$  exhibits a very low current under the experimental conditions described in Figure 1. For example, the platinum oxide reduction peak was  $50\text{ }\mu\text{A}$  high. The potential of ring electrode, where oxidation of both species can be detected, was set to  $0.6\text{ V}$ .

The collection efficiency,  $N_{\text{eff}}$ , of a RRDE is defined as:

$$N_{\text{eff}} = \frac{I_{\text{R}} n_{\text{D}}}{I_{\text{D}} n_{\text{R}}}$$

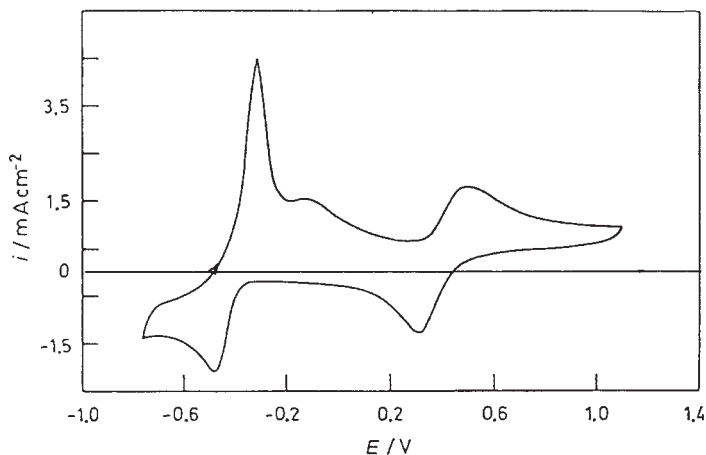


Figure 1. Cyclic voltammograms at a sweep rate of  $50\text{ mV s}^{-1}$  on a quiescent platinum disc electrode of  $0.1\text{ mol dm}^{-3}\text{ Ni}^{2+}$  and  $0.1\text{ mol dm}^{-3}\text{ Fe}^{2+}$  in  $0.5\text{ mol dm}^{-3}\text{ Na}_2\text{SO}_4$  adjusted to pH 2.7.

where  $I_D$  and  $I_R$  are disc and ring currents, respectively,  $n_D$  and  $n_R$  are numbers of electrons exchanged in the electrode reactions on disc and ring electrodes, respectively. The collection efficiency for this electrode configuration was calculated and confirmed experimentally.<sup>5</sup> The value of 0.2 was obtained by the use of  $I_2/I^-$  redox couple in  $0.5 \text{ mol dm}^{-3} \text{ H}_2\text{SO}_4$ .

### Surface Analysis

The XPS measurements were carried out on  $0.8 \times 0.8 \text{ cm}$  stainless steel-304 plates. The electrodes were emersed from sodium hydroxide solution at 0.5 V, the untreated electrode after 1.5 cycles between  $-1.2$  and  $0.5 \text{ V}$  and the electrochemically treated electrodes after 30.5 cycles within the same potential range. The electrodes were washed, dried in desiccator under low vacuum conditions, and transferred into the ultrahigh vacuum chamber of the spectrometer. The spectrometer consists of a hemispherical analyzer (Vacuum Science Workshop HA 100) and a Mg/Al dual-anode X-ray source. The excitation energy was  $1253.6 \text{ eV}$  (Mg  $K\alpha$  line).

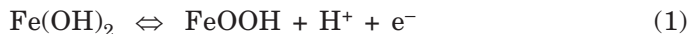
### Oxide Growth

The oxide was grown by cycling voltammetry between  $-1.2 \text{ V}$  and  $0.5 \text{ V}$  at  $50 \text{ mV s}^{-1}$  in  $1 \text{ mol dm}^{-3} \text{ NaOH}$  solution (Fluka *puriss. p.a.*) using an EG&G 273/97 potentiostat/galvanostat. The electrode that has passed only one potential sweep will be in further text referred to as an untreated electrode, while the electrode subjected to 30 cyclic voltammograms will be referred to as a modified electrode.

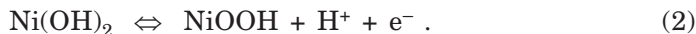
## RESULTS AND DISCUSSION

### Optimum Conditions for Oxide Growth

The efficiency of oxide growth was determined as a function of potential limits, sweep rate, frequency and number of cycles. The cyclic voltammograms presented in Figure 2 show the development of two pairs of peaks, between  $-1.1$  and  $-0.7 \text{ V}$ , and between  $0.3 \text{ V}$  and  $0.5 \text{ V}$ , respectively. On the basis of previous results obtained by the use of single metal components, nickel<sup>6-8</sup> and iron,<sup>9-11</sup> peaks which exhibit an increase in current under the conditions of cyclic voltammetry between  $-1.1 \text{ V}$  and  $-0.5 \text{ V}$  are attributed to the Fe(II)/Fe(III) oxidation/reduction process:<sup>9</sup>



while the peaks between  $0.3 \text{ V}$  and  $0.5 \text{ V}$  correspond to the Ni(II)/Ni(III) redox process:<sup>6</sup>



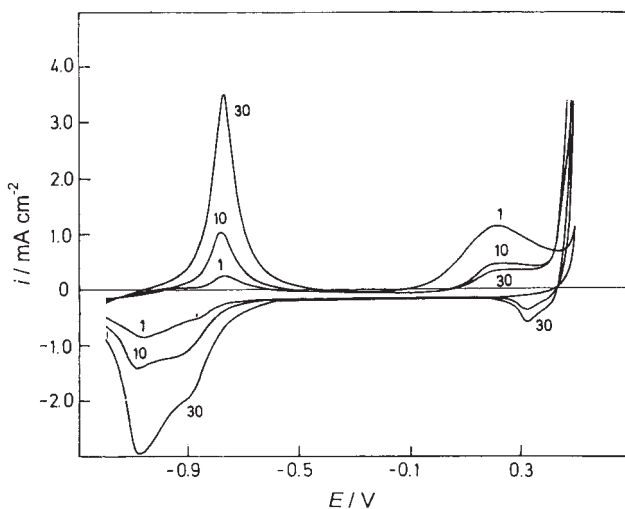


Figure 2. Cyclic voltammograms at a sweep rate of  $50 \text{ mV s}^{-1}$  from  $-1.2 \text{ V}$  to  $0.5 \text{ V}$  of the stainless steel-304 electrode in  $1 \text{ mol dm}^{-3} \text{ NaOH}$  during the 1st, the 10th and the 30th cycles from  $-1.2 \text{ V}$  to  $0.5 \text{ V}$  at  $50 \text{ mV s}^{-1}$ .

The peak in positive direction at  $0.25 \text{ V}$ , which decreases during potential cycling, is attributed to chromium oxidation.

The voltammetric charge of the anodic peak at  $-0.8 \text{ V}$  was chosen as the measure of the efficiency of oxide growth. The optimum lower potential limit was obtained at negative potentials in the hydrogen evolution region, (Figure 3a). Upper potential limit exhibited different behaviour. The optimum oxide growth was achieved when positive potential limit was set to  $0.5 \text{ V}$  (Figure 3b).

The efficiency of oxide growth as a function of sweep rate shows almost constant values up to  $50 \text{ mV s}^{-1}$ , when it starts to decrease. Consequently, in the trade-off between efficiency and experimental time consumption, the optimum sweep rate was found to be  $50 \text{ mV s}^{-1}$  (Figure 4a). The voltammetric charge increases with the increase of the number of cycles. It reaches a plateau at about  $30 \text{ mQ cm}^{-2}$  after 200 cycles (Figure 4b).

#### *Stability of the Alloy during Oxide Growth under Cyclic Voltammetric Conditions in Alkaline Solution*

The rotating ring-disc electrode was used in monitoring the stability of oxide growth during potential cycling of the stainless steel-304 electrode in  $1 \text{ mol dm}^{-3} \text{ NaOH}$  solution. The disc electrode was potentiodynamically po-

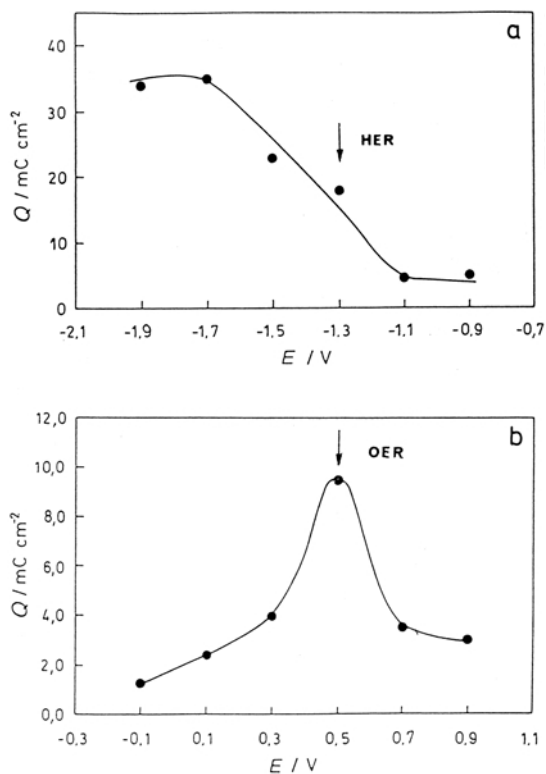


Figure 3. Charge capacity associated with the first anodic peak at  $-0.8$  V (Figure 2) as a function of the lower limit of the potential sweep after 30 cycles at  $50 \text{ mV s}^{-1}$  in  $1 \text{ mol dm}^{-3}$  NaOH. The upper limit was fixed at  $0.5$  V (a); and charge capacity as a function of the upper limit of the potential sweep. The lower limit was fixed at  $-1.2$  V (b). The analytical cyclic voltammogram was recorded at  $50 \text{ mV s}^{-1}$  from  $-1.2$  V to  $0.5$  V. The arrows denote the commencements of the hydrogen evolution reaction (HER) and oxygen evolution reaction (OER), respectively.

larized between the same potential limits as the electrodes used in oxide growth (Figure 2). Figure 5 shows ring currents during potential cycling of the stainless steel-304 electrode, more precisely, during one full cycle from  $-1.2$  V to  $0.5$  V and back to  $-1.2$  V. Two cycles, the 1st and the 30th, were monitored by RRDE. As it can be seen in Figure 2, the starting potential of the cyclic voltammogram is at a potential value where a small negative current due to hydrogen evolution occurs. The corresponding response on the ring electrode (Figure 5) is a decrease in current during the first 2–3 seconds due to hydrogen ionization. The peak after 8 s, *i.e.* at  $-0.8$  V, corresponds to  $\text{Fe}(\text{OH})_2$  oxidation (Figure 2). Therefore, a part of  $\text{Fe}(\text{OH})_2$  layer dissolves during potential cycling. The voltammetric charge of the stainless

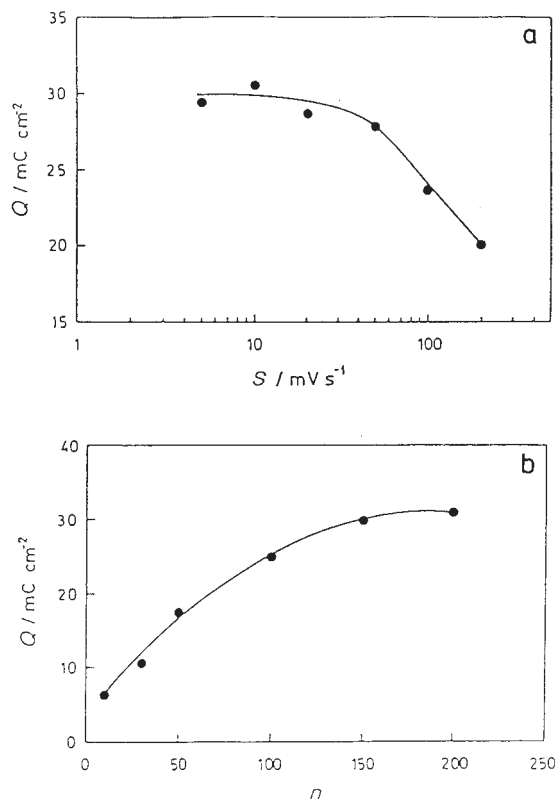


Figure 4. Charge capacity associated with the first anodic peak at  $-0.8$  V (Figure 2) as a function of sweep rate in  $1 \text{ mol dm}^{-3}$  NaOH on an oxide film on which an oxide was previously grown by 150 cycles at  $50 \text{ mV s}^{-1}$  (a); and charge capacity as a function of the number of cycles (b). The analytical cyclic voltammograms used for charge integration were recorded at  $50 \text{ mV s}^{-1}$  from  $-1.2$  V to  $0.5$  V in both pictures.

steel-304 disc electrode of the above reaction after 30 cycles is  $10.7 \text{ mC cm}^{-2}$  (Figure 4b). The corresponding ring charge was obtained by integration of the ring current between 3 and 20 seconds in Figure 5. This charge is  $6.0 \mu\text{C}$  during the 30th cycle. Taking into account the collection efficiency 0.2 and normalization of data for voltammetric charge in Figure 4b (unit area) to a geometrical area of the disc electrode ( $0.2 \text{ cm}^2$ ), the corresponding charge was multiplied by 25. Therefore, the oxide dissolution charge is  $150 \mu\text{C cm}^{-2}$ . This is 1.4% of the total anodic current on the disc electrode, in other words 1.4% of the anodic current is due to iron dissolution. Further analysis of the ring current shows that the oxide film is very stable during the cycling between  $-0.2$  V and  $-0.75$  V before reaching iron reduction at  $-0.8$  V. There is a small peak between  $0.3$  V and  $0.5$  V, which corresponds to Ni(II)

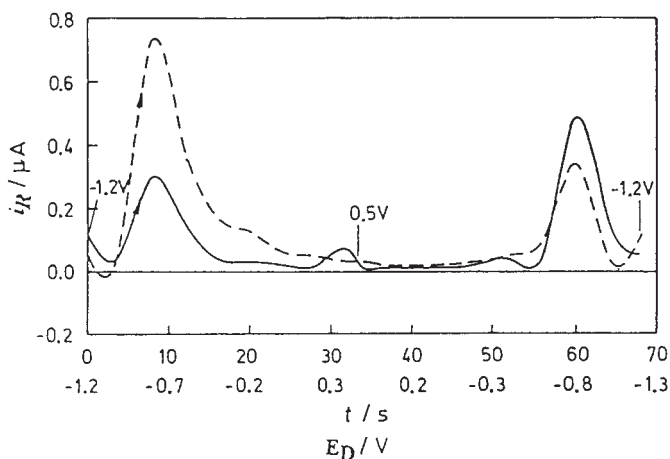


Figure 5. Ring current-time (potential) curves during the potential scan of the stainless steel-304 disc electrode at a sweep rate of  $50 \text{ mV s}^{-1}$  in  $1 \text{ mol dm}^{-3}$  NaOH solution. Untreated electrode (full line), modified electrode by 30 cycles (dashed line). The ring potential was at  $0.4 \text{ V}$ .

oxidation. It is interesting that the thick oxide film formed after 30 cycles is even more stable in this potential range when compared to the oxide of the first cycle. This is also the case in the potential range of iron and nickel reduction during the backward scan at  $-0.8 \text{ V}$ . It should be pointed out that the oxide film either in its initial stage of formation or in its grown stage is not completely stable during the cycling. There is a small current below  $0.1 \text{ } \mu\text{A}$  which shows continuous dissolution during the cycling.

#### *Stability of the Grown Oxide Film in Acid Solution*

Two electrodes, the untreated and the modified one, when transferred to an acid solution, exhibit different properties in their corrosive behaviour. Figure 6 shows open-circuit potential-time curves obtained by the untreated electrode and the electrode modified by the previously grown oxide film. The potential of the untreated electrode decreased after  $1000 \text{ s}$  to the active corrosion potential of  $-0.3 \text{ V}$ . The potential of the modified electrode was still in the passive state after 1 hour. The question is which part of the oxide is responsible for the enhanced stability. It is well known that the enhanced stability of chromium containing iron and nickel-based alloys change their properties from iron-like to chromium-like behaviour when the chromium content exceeds  $10\%$ .<sup>12</sup> Chromium oxide species stabilize the surface against corrosion. However, the situation is somewhat different for electrodes modified by the growth of hydrous oxide film under the conditions of

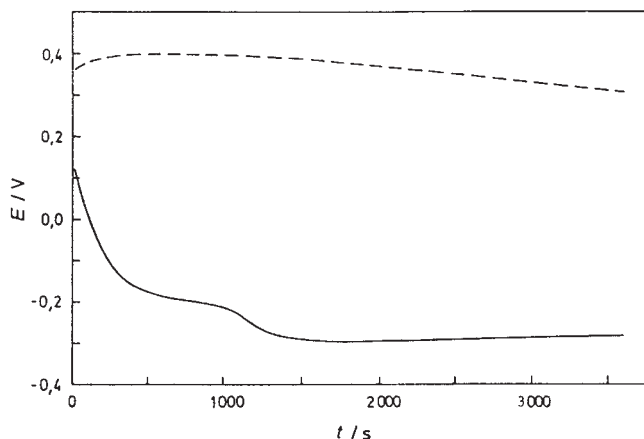


Figure 6. The potential of open-circuit in  $0.5 \text{ mol dm}^{-3} \text{ H}_2\text{SO}_4$  of untreated stainless steel-304 electrode (full line), and after 30 cycles from  $-1.2 \text{ V}$  to  $0.5 \text{ V}$  in  $1 \text{ mol dm}^{-3} \text{ NaOH}$  (dashed line).

repetitive potential cycling obtained in this work than for not treated electrodes. In the former case, a deeper penetration into the alloy's structure is achieved, accompanied by the presence of a greater amount of iron and nickel atoms available for dissolution. The selective dissolution of iron and nickel in acid solution was detected voltammetrically in the case of stainless steel-302, and by X-ray photoelectron spectroscopy (XPS) measurements in the case of inconel-600, modified in the same way as stainless steel-304 in the present work.<sup>2,3</sup> The present paper shows the quantity of dissolved oxide species during the cycling of the stainless steel-304 electrode (Figure 5) and the kinetics of its dissolution (Figure 7).

Figure 7 shows RRDE measurements when the electrodes, untreated and modified ones, were transferred to an acid solution of pH 2.7. After 5 s, the oxide film was dissolved in the case of unmodified electrode (the 1st cycle), and after 15 s in the case of the grown oxide film. The ring currents reached zero value, and this means that both iron and nickel were dissolved from the grown hydrous part of the stainless steel-304. The overall stability of the oxide film was not lost. The cyclic voltammogram of the modified electrode, which was previously immersed for 24 hours in  $0.5 \text{ mol dm}^{-3} \text{ H}_2\text{SO}_4$  (Figure 8), shows disappearance of iron and nickel peaks while the electrode was transferred to  $1 \text{ mol dm}^{-3} \text{ NaOH}$  solution. The dissolution occurred within 15 s, as shown previously by the use of RRDE. However, open-circuit potential measurements in acid solution (Figure 6) show that, despite dissolution of these metals from the surface layer, the electrode was still in the passive region without active dissolution from the alloy's surface.

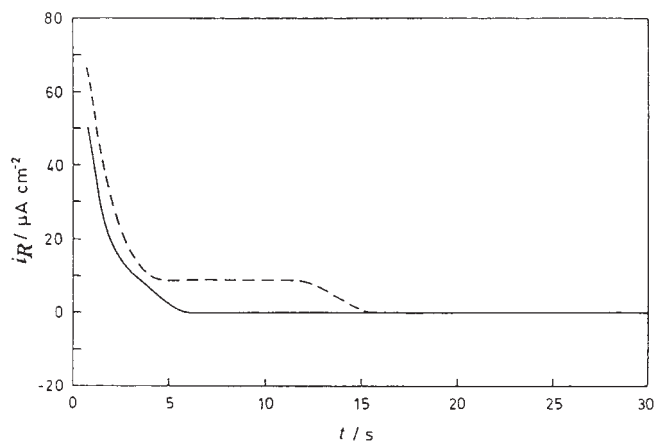


Figure 7. Ring current-time curves in  $0.1 \text{ mol dm}^{-3} \text{ Na}_2\text{SO}_4$  solution adjusted to pH 2.7 of the untreated stainless steel-304 disc electrode (full line); and of the stainless steel-304 disc electrode cycled 30 times between  $-1.2 \text{ V}$  and  $0.5 \text{ V}$  in  $1 \text{ mol dm}^{-3} \text{ NaOH}$  (dashed line). Rotation speed 2500 rpm. The disc electrode was held at open circuit, and the ring electrode was at  $0.6 \text{ V}$ .

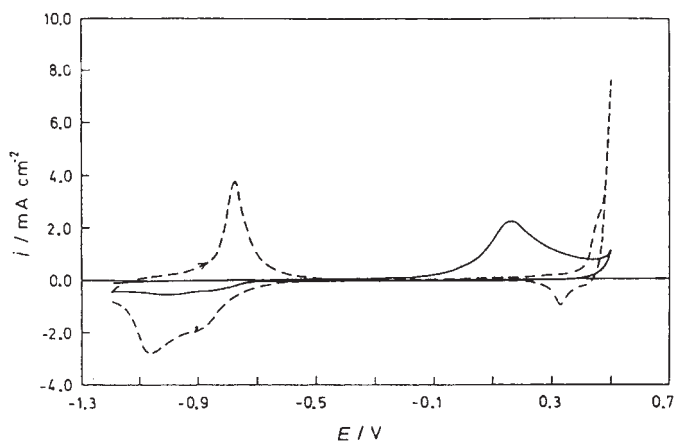


Figure 8. Cyclic voltammograms at a sweep rate of  $50 \text{ mV s}^{-1}$  in  $1 \text{ mol dm}^{-3} \text{ NaOH}$  of the stainless steel-304 electrode after the electrode was previously modified by 30 cycles in  $1 \text{ mol dm}^{-3} \text{ NaOH}$  (dashed line), and the same electrode after immersion in  $0.5 \text{ mol dm}^{-3} \text{ H}_2\text{SO}_4$  for 24 hours (full line).

### Surface Analysis

The XPS spectra of the 2p levels of the three constituents of the stainless steel-304 taken before and after surface modifications are shown in

Figure 9. The shift of  $2p_{3/2}$  levels towards higher binding energy in the case of all three elements, Fe, Ni and Cr, after electrochemical modification by cyclic voltammetric treatments, evidences the increase in their oxidation states. Moreover, a decrease in intensities of Fe  $2p_{3/2}$  and Ni  $2p_{3/2}$  levels sup-

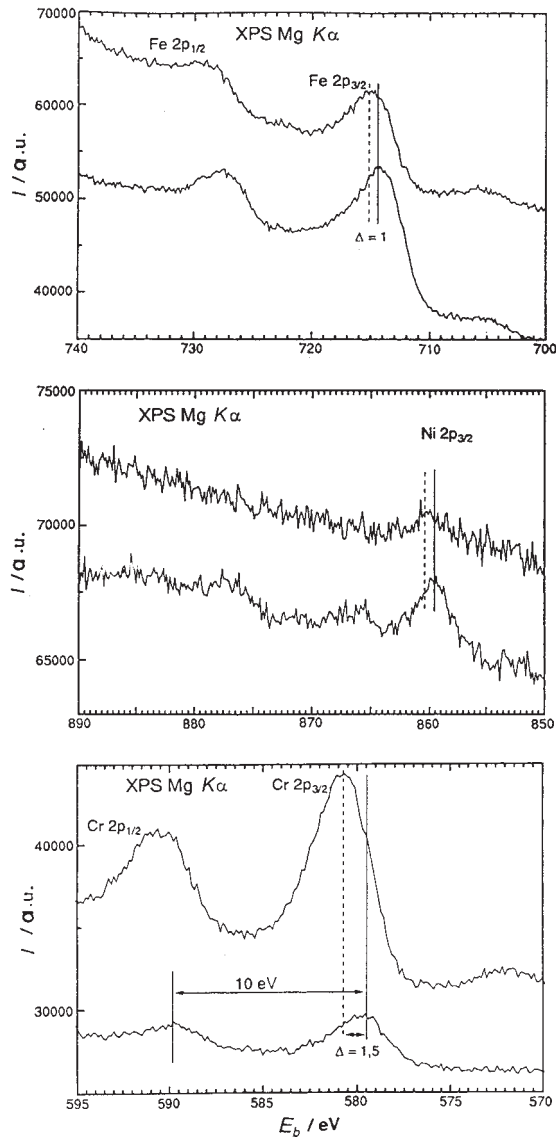


Figure 9. XP spectra of the 2p levels of Fe, Ni and Cr before (lower spectra) and after electrochemical treatment (upper spectra).

ports previous findings by cyclic voltammetry and RRDE of their selective dissolution, while the significant increase of Cr 2p<sub>3/2</sub> evidences the enrichment in chromium in the modified layer.

### *The Modified Oxide Film Model*

Three models proposed in the literature for the electrochemical behaviour of metal oxides and passive oxide films have been chosen and used together with experimental facts presented in this paper to explain the enhanced stability of the modified stainless steel-304 surface oxide layer. The first model describes hydrous oxide films grown on Rh, Ir, Fe and under the conditions of repetitive potential cycling.<sup>1</sup> Hydrous oxides are porous, highly hydrated with specific density much lower (about 2 g cm<sup>-3</sup>) when compared to anhydrous oxides (about 12 g cm<sup>-3</sup>).<sup>1</sup> The second model is the polymeric hydrated oxide model for the passivity of iron and stainless steels.<sup>13-16</sup> This model implies the significant role of water in the stability of passive film. Water, hydroxide and oxy-hydroxide species link metal atoms together and protect them from dissolution. The third model is a percolation model for the passivity of stainless steels which implies that, after selective dissolution of nickel and iron, the surface remains enriched in chromium.<sup>17-19</sup>

The model that we propose in this work unifies the above described procedures in so far as: i) the cyclic voltammetric modification forms a hydrous oxide film (model 1) in which a deeper penetration into the alloy bulk is achieved; ii) the density of hydrous oxide layer indicates the presence of water within the structure (model 2), and iii) the selective dissolution of Fe and Ni leaves the surface layer enriched in Cr (model 3).

In our model for the enhanced stability of stainless steel-304, after its modification in the alkaline solution followed by its transfer to acid solution, the protective layer is thicker than the ones either described by the other models or spontaneously formed in the air. The following experimental evidences support the model that we propose. Undoubtedly, the hydrous oxide film was grown by potential cycling in alkaline solution, as evidenced by the significant increase in voltammetric charge of iron and nickel oxidation, in the same way as the film grows on single components of stainless steels, nickel and iron. The selective dissolution of iron and nickel was proven in the present paper by RRDE, by the shape of the cyclic voltammogram (Figure 8), and by XPS measurements (Figure 9). The cyclic voltammogram (Figure 8) shows disappearance of iron and nickel oxidation/reduction peaks, while Figure 9 shows a decrease of XPS Ni 2p<sub>3/2</sub> and Fe 2p<sub>3/2</sub> levels and enrichment of chromium exhibited through the increase of Cr 2p<sub>3/2</sub> level. The layer consists of enriched chromium content in the Cr-O-Cr chains, which were formed after selective dissolution of iron and nickel in acid solution.

## CONCLUSIONS

The hydrous oxide growth on stainless steel-304 can be achieved under the conditions of cycling voltammetry in alkaline solution. The oxide dissolves during the cycling; however, only 1.4% of Fe(II) was dissolved in the potential range of  $\text{Fe}(\text{OH})_2/\text{FeOOH}$  oxidation/reduction process. The rest of the charge was consumed in the formation of a stable oxide film. A more stable oxide layer can be formed by the growth of a thick hydrous oxide in alkaline solution and its partial dissolution of iron oxide and nickel oxide species in an acid solution. The layer remains enriched in chromium, with enhanced protection against hydronium ions.

*Acknowledgements.* – This work was supported by the Ministry of Science and Technology of the Republic of Croatia (Grants 00981507 and 00350108). The technical assistance of Momir Milunović, B. Sc., and Mr. Srećko Karašić is gratefully acknowledged.

## REFERENCES

1. L. D. Burke and M. E. G. Lyons, *Electrochemistry of Hydrous Oxide Films*, in: *Modern Aspects of Electrochemistry*, No 18, R. E. White, J. O'M. Bockris, and B. E. Conway (Eds.), Plenum Press, New York, 1986, pp. 169–248.
2. M. Vuković, *Corros. Sci.* **37** (1995) 111–120.
3. D. Marijan, M. Vuković, P. Pervan, and M. Milun, *J. Appl. Electrochem.* **28** (1998) 96–102.
4. H. H. Uhlig, *Corrosion and Corrosion Control*, John Wiley, New York, 1963.
5. M. Vuković, *J. Chem. Soc., Faraday Trans. I* **86** (1990) 3743–3746.
6. L. D. Burke and D. P. Whelan, *J. Electroanal. Chem.* **109** (1980) 385–388.
7. L. D. Burke and T. A. M. Twomey, *J. Electroanal. Chem.* **162** (1984) 101–119.
8. A. Visintin, A. C. Chialvo, W. E. Triaca, and A. J. Arvia, *J. Electroanal. Chem.* **225** (1987) 227–239.
9. L. D. Burke and O. J. Murphy, *J. Electroanal. Chem.* **109** (1980) 379–383.
10. L. D. Burke and M. E. G. Lyons, *J. Electroanal. Chem.* **198** (1986) 347–368.
11. O. A. Albani, J. O. Zerbino, J. R. Vilche, and A. J. Arvia, *Electrochim. Acta* **31** (1986) 1403–1411.
12. H. Kaesche, *Die Korrosion der Metalle*, Springer-Verlag, Berlin, 1979.
13. G. Okamoto, *Corros. Sci.* **13** (1973) 471–489.
14. W. E. O'Grady and J. O'M. Bockris, *Surf. Sci.* **38** (1973) 249–255.
15. R. W. Revie, B. G. Baker, and J. O'M. Bockris, *J. Electrochem. Soc.* **122** (1975) 1460–1466.
16. W. E. O'Grady, *J. Electrochem. Soc.* **127** (1980) 555–563.
17. K. Sieradzki and R. C. Newman, *J. Electrochem. Soc.* **133** (1986) 1979–1980.
18. R. C. Newman, Fooung Tuck Meng, and K. Sieradzki, *Corros. Sci.* **28** (1988) 523–527.
19. S. Quian, R. C. Newman, R. A. Cottis, and K. Sieradzki, *J. Electrochem. Soc.* **137** (1990) 435–439.

## SAŽETAK

**Površinska modifikacija elektrode od nehrđajućeg čelika 304.****1. Studije voltametrijom, rotirajućom disk-elektrodom s prstenom i XPS**

*Dražen Marijan, Marijan Vuković, Petar Pervan i Milorad Milun*

Pod uvjetima uzastopne promjene potencijala u NaOH ( $1 \text{ mol dm}^{-3}$ ) postignut je rast hidratiziranog oksidnog filma na elektrodi od nehrđajućeg čelika 304. Anodna voltametrijska struja oksidacije željeza upotrijebljena je kao mjera rasta oksida u ovisnosti o granicama potencijala, o brzini promjene potencijala i o broju ciklusa. Stabilnost oksidnog sloja bila je praćena upotrebom rotirajuće disk-elektrode s prstenom. Nađeno je da za vrijeme cikliziranja potencijala u lužnatoj otopini 1,4% ukupnog anodnog naboja odgovara reakciji otapanja željeza. Selektivno otapanje željeza i nikla, na prethodno naraslom oksidnom sloju u lužnatoj otopini, praćeno je u kiseloj sredini na  $\text{pH} = 2,7$ . Predložen je model povećane stabilnosti hidratiziranog oksidnog sloja u kiseloj otopini. Model je zasnovan na voltametrijskim podacima, na mjerenjima s rotirajućom elektrodom s prstenom, te na površinskoj analizi fotoelektronskom spektroskopijom X-zraka, podrazumijeva da se nakon rasta hidratiziranog oksidnog sloja cikliziranjem potencijala u lužnatoj otopini, sloj obogaćuje kromom zbog selektivnog otapanja željeza i nikla. Lanci Cr-O-Cr stabiliziraju modificirani sloj i pridonose povećanju otpornosti na koroziju. Taj model objedinjuje nekoliko prethodno opisanih modela: model rasta hidratiziranih oksidnih filmova cikliziranjem potencijala, model polimernog hidratiziranog oksida u pasivnosti željeza i nehrđajućih čelika, te model obogaćivanja u pasivnosti nehrđajućeg čelika.